Available online at www.sciencedirect.com
SCIENCE DIRECT®
ELSEVIER
Nuclear Instruments and Methods in Physics Research A 522 (2004) 477–486
NUCLEAR INSTRUMENTS & METHODS IN PHYSICS RESEARCH Section A
www.elsevier.com/locate/nima

Development of a new photomultiplier tube with high sensitivity for a wavelength-shifter fiber readout

M. Itaya[a,1], T. Inagaki[b], T. Iwata[a], G.Y. Lim[b], H. Oishi[c], H. Okuno[b], Y. Tajima[a], H.Y. Yoshida[a,*], Y. Yoshimura[b]

[a] *Department of Physics, Yamagata University, 1-4-12 Kojirakawa-machi Yamagata 990-8560, Japan*
[b] *High Energy Accelerator Research Organization (KEK), Tsukuba, Ibaraki 305-0801, Japan*
[c] *Hamamatsu Photonics K.K., Shizuoka 438-0193, Japan*

Received 24 July 2003; accepted 5 November 2003

Abstract

We have developed a new photomultiplier tube (PMT) with high sensitivity for a wavelength-shifter fiber readout of plastic scintillators. Improvements of the photoelectron yield were made on a 2-in. PMT (Hamamatsu R329) by adopting (1) a prism-shaped photocathode, (2) an extended-green photocathode material, and (3) an optical mirror surface of the electrodes. As a result, the number of photoelectrons obtained by the new PMT has increased to be 1.8-times that by R329. Other PMT characteristics, such as uniformity of sensitivity, time response and darkcurrent are not so much different from those of R329 for practical applications.
© 2003 Elsevier B.V. All rights reserved.

PACS: 29.90.+r; 29.40.Mc; 29.40.Vj

Keywords: Photomultiplier tube (PMT); Prism photocathode; Wavelength-shifter (WLS) fiber readout; Quantum efficiency (QE); Time response; Darkcurrent

1. Introduction

KEK-PS E391a is an experiment to study direct CP violation through a measurement of the $K_L \to \pi^0 \nu\bar{\nu}$ decay branching ratio [1,2]. The signature of the decay mode is 2γ, of which the invariant mass is consistent with π^0 and nothing other than one π^0. This requires a photon veto counter system with a high efficiency that covers the whole K_L decay region.

Lead-scintillator sandwich-type counters were designed for this purpose [2]. One of them is a central-barrel veto counter with a length of 5.5 m; another is a front-barrel veto counter with a length of 2.75 m. They are made of 60 layers of 5 mm-thick extruded plastic scintillators and thin lead sheets. Wavelength-shifter (WLS) fibers of 1 mm in diameter embedded in grooves on the plastic scintillator surface are employed for a scintillation light readout. A similar system was adopted and

*Corresponding author. Tel.: +81-23-628-4570; fax: +81-23-628-4567.
E-mail address: yoshida@sci.kj.yamagata-u.ac.jp (H.Y. Yoshida).
[1] Present address: NEC TOKIN Corp., 7-1, Kohriyama 6-chome, Taihaku-ku, Sendai-shi, Miyagi 982-8510, Japan

0168-9002/$ - see front matter © 2003 Elsevier B.V. All rights reserved.
doi:10.1016/j.nima.2003.11.201

developed in the BNL experiment E926(KOPIO) which has the same physics goal [3,4]. There are several advantages in this choice. The convenient readout with the WLS fibers leads to reducing the number of photomultiplier tubes (PMTs), hence resulting in low cost. Such a readout allows a uniform detector response over the whole detector area, because the attenuation length of the WLS fibers is sufficiently longer than that of the plastic scintillators. However, there is a drawback of a poor light yield at the PMT. To secure the strength of the counter structure, we adopted a MS (methyl-methacrylate styrene) resin based scintillator produced by the extrusion technique. It provides a less light yield than that of other plastic scintillators commonly used, e.g. Bicron BC408 [5]. In addition to this, such a WLS fiber readout system has a lower light collection efficiency than that of an ordinary acrylic light guide system. In order to overcome this, we made a new attempt to increase the photoelectron yield by making improvements on the PMT. We report on these improvements and the application of the new PMT for the WLS fiber readout.

2. Improvements on the R329 PMT

We employed a 2-in. PMT, Hamamatsu R329 [6], considering cost, easy handling and the size of the WLS fiber bundles. The specifications of the R329 PMT are summarized in Table 1.

Table 1
Specifications of the Hamamatsu R329 PMT [6]

Spectral response	300−650 nm
Wavelength of maximum response	420 nm
Photocathode material	Bialkali
Photocathode minimum effective area	46 mm ϕ
Window material	Borosilicate glass
Window shape	Plano-concave
Dynode structure	Linear focused
Dynode number of stages	12
Gain	1.1×10^6 at 1500 V
Maximum supply voltage	2700 VDC
Electron transit time	48 ns
Transit time spread	1.1 ns

The improvements made on this PMT were as follows:

(1) Prism-shaped photocathode: The inner surface of the photocathode window was molded into a prism-shape, as shown in Fig. 1. This processing gives a longer passage of the light through the photocathode material, resulting in an increase of the chance for photoelectric emission. The thickness of the photocathode material was kept the

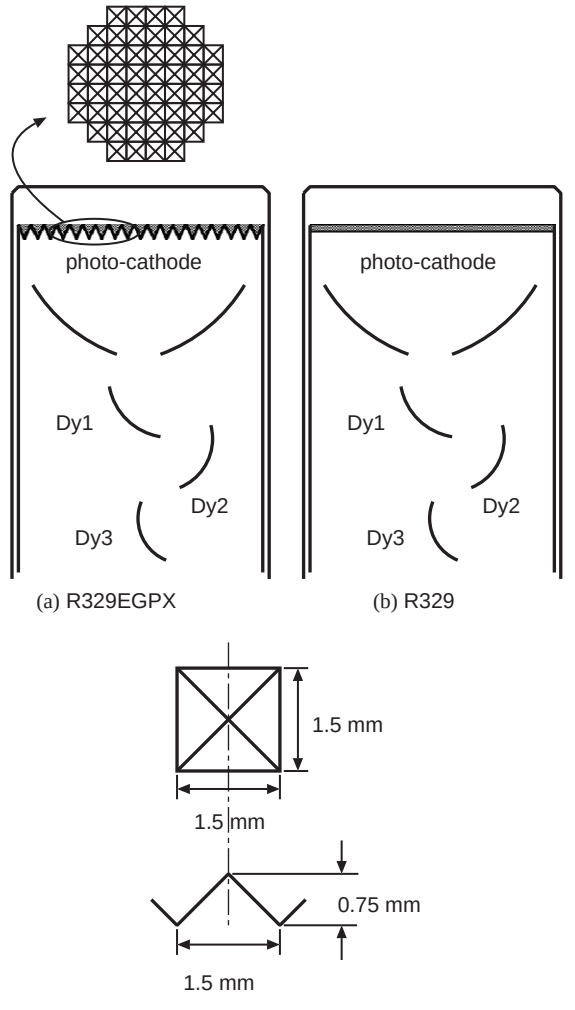

Fig. 1. Schematic structure of (a) the new PMT (R329EGPX); (b) the standard PMT (R329). The photocathode of the new PMT has 827 prisms on its surface. The thickness of photocathode material is the same for both PMTs; (c) structure of each prism.

same as that of the standard PMT. Since the angle of the surface of the prisms is inclined by 45°, it is expected that the chance of photoelectric emission is increased by a factor of $\sqrt{2}$ for light with a normal incidence on the window surface of the PMT.

(2) Extended-green photocathode: The photocathode material was changed into the so-called extended-green one. By changing the mixture of the contents of the photocathode material, its work function was lowered. This extends its sensitive region to 450−600 nm, which matches the emission spectrum of the WLS fiber.

(3) Well-polished electrodes inside the PMT: The surface of the focusing electrode, the first and the second dynodes, was polished to have better light reflection. The light, having passed through the photocathode, and hence not having contributed to the photoelectric effect, is reflected on the surface back to the photocathode. Although the probability of the photoelectric effect is expected to be somewhat increased by this improvement, a quantitative evaluation was not performed.

The quantum efficiencies (QE) of the PMTs at different wavelengths were measured by Hamamatsu Photonics K.K., as shown in Fig. 2(a) [7]. The emission spectrum of the WLS fiber (Kuraray Y-11) is also shown in Fig 2(b) as a reference. The standard bialkali-photocathode PMTs, R329, give the maximum QE at around 400 nm. The PMTs with the extended-green photocathode (hereafter denoted as "extended-green PMTs"), R329EG, give higher values at longer wavelengths, as expected. They give an improvement by a factor of 1.0–1.4 at 450−600 nm, which corresponds to the wavelength of the emission from the WLS fiber. The value of QE of the new PMTs, R329EGPX, is increased compared to those of the extended-green ones over the whole region above 400 nm. In particular, above 600 nm, an unexpected enhancement is seen. This is one of preferable features for applications with WLS fibers. Below 400 nm, however, the new PMTs are not as good as expected; the value at 350 nm is about one order of a magnitude less than those of the other PMTs. This is due to the effect of the different window material. The window of the new PMT is made of a kind of borosilicate glass, but is slightly changed from that of ordinary R329 to be suitable for making the prism structure in a molding press. Also, this material has a worse transmission below 400 nm compared with that used in the standard PMTs. However, it will not cause any problems in our application with the WLS fibers (Bicron BCF-91A and Kuraray Y-11), having a peak in the region 450−600 nm in their emission spectrum, as shown in Fig. 2(b).

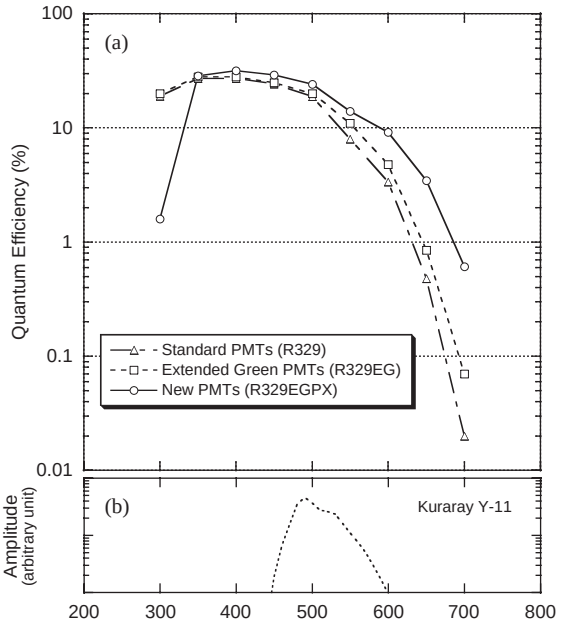

Fig. 2. (a) The QEs measured at different wavelengths. The open triangles represent the data for the standard PMTs (R329), the open squares for the extended-green ones (R329EG) and the open circles for the new ones (R329EGPX). Note that the data represent the averaged values obtained with 19 pieces of R329, 3 pieces of R329EG and 9 pieces of R329EGPX; (b) the emission spectrum of the WLS fiber, Kuraray Y-11, to be used in the E391a experiment. The spectrum was obtained for excitation at a wavelength of 400 nm using a fluorescence spectrometer, Hitachi F-4500. It was confirmed that another WLS fiber to be used in the experiment, Bicron BCF-91A, gives a similar emission spectrum.

Regarding the above-mentioned improvements, we expect an increase of the photoelectron yield by at least a factor of 1.7 in the region of the emission spectrum of the WLS fiber. To confirm this increase of the photoelectron yield, we made tests with the actual counter in the WLS fiber readout.

We report on the methods of the tests and their results in subsequent sections.

3. Photoelectron yield in a WLS fiber readout

The photoelectron yield of the new PMTs was investigated for an actual read out with the WLS fiber in the setup shown in Fig. 3, and compared with that of the standard PMTs. A WLS fiber (Kuraray Y-11) of 1 mm diameter, 5.2 m in length is embedded in the groove on the surface of the Bicron BC408 plastic scintillator (100 mm × 50 mm × 5 mm). It guides the secondary light to the center of the PMT's window. The plastic scintillator is exposed to β-rays from ^{106}Ru, and the signal pulse height is registered by ADC, as shown in Fig. 4. The ADC is gated by the signal from a trigger counter mounted above the plastic scintillator.

The ADC spectrum was fitted by the resolution convoluted Poisson distribution [8],

$$F(x) = A \sum_{N=1}^{N=N_{\max}} \frac{e^{-\bar{N}}\bar{N}^N}{N!} \frac{1}{\sqrt{2\pi N}\sigma} \times \exp\left\{-\frac{(x - pN - q)^2}{2N\sigma^2}\right\}$$

where x is the ADC channel, A is the normalization factor, $\bar{N}$ is the average number of photoelectrons (p.e.), σ is the single-photoelectron peak resolution, p is the peak interval and q is the pedestal channel. In these fittings, A, $\bar{N}$, σ and p are the free parameters to be determined from the obtained spectrum. From the single-photoelectron peak measurement for each PMT, we have also confirmed the σ and p values. The obtained value of $\bar{N}$ has an uncertainty of ~3%, besides the fitting error of 1–2%. The uncertainty is due to selection of the fitting range; in particular, the position of the lower edge affects the fitting, because the spectrum in the lower channel range may be slightly contaminated with the background due to electrical noises, and so on.

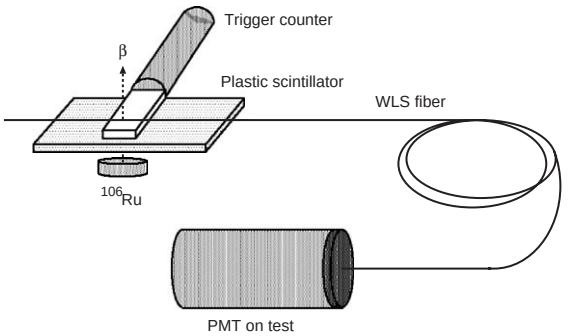

Fig. 3. Experimental setup for measuring the number of photoelectrons.

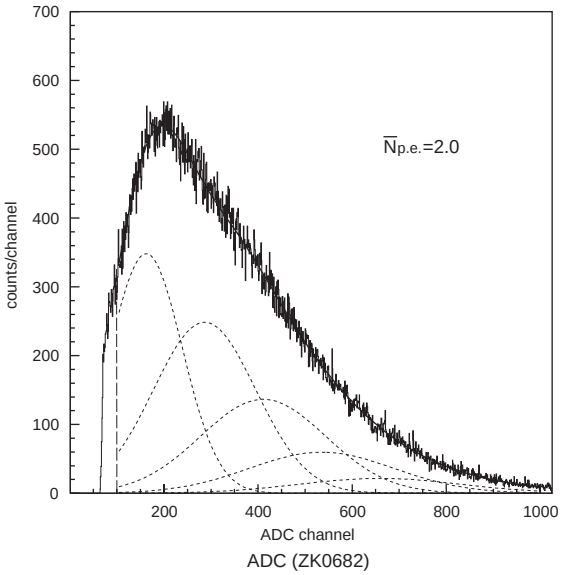

Fig. 4. Typical ADC spectrum obtained with the new PMT. The solid curve is the result of the fit described in the text. The dotted curves are decomposed Gaussians for $N = 1, 2, 3, 4, 5$.

The averaged numbers of photoelectrons obtained with the PMTs operated at 2.2 kV are shown in Fig. 5. It turned out that the new PMTs give about a 1.8-times larger photoelectron yield than the standard ones. The results for the extended-green PMTs show that the photoelectron yield is about 1.5-times larger than that of the standard PMT. Hence, the adoption of a prism-shaped photocathode and the polished electrodes improve the photoelectron yield by a factor of 1.2. This improvement is crucial as well as the extended-green photocathode in order to overcome the disadvantage of using the MS resin based scintillator which provides a light yield of

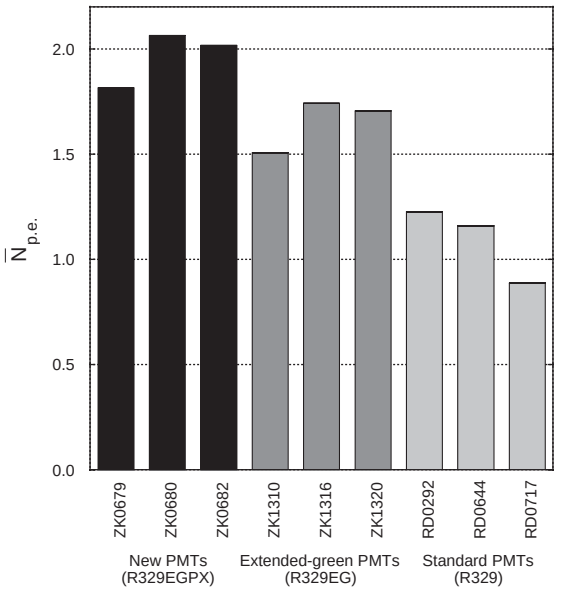

Fig. 5. Averaged numbers of photoelectrons obtained with the new PMTs (ZK0679, ZK0680, ZK0682), the extended-green ones (ZK1310, ZK1316, ZK1320) and the standard ones (RD0292, RD0644, RD0717).

70–80% of the Bicron BC408. Comparing with the standard PMTs in combination with the Bicron BC408, the new PMTs are expected to give a more photoelectron yield, at least by a factor of 1.26 ($= 0.7 \times 1.8$), in combination even with the MS resin-based scintillator.

In addition to the uncertainty in the fitting procedure mentioned above, another uncertainty of $\sim$4% is caused by the reproducibility of the experimental condition, e.g. positioning of the PMTs and the WLS fiber in the setup. Taking this into account, the total uncertainty in the photoelectron yield is estimated to be at most 8%. Even taking into account the uncertainty, the observed differences of the photoelectron yield among the different types of PMT are significant.

4. Uniformity of sensitivity

The structure of the prism-shaped photocathode may influence the uniformity of the sensitivity. As reported by Hamamatsu Photonics K.K. [9], a fine variation in its sensitivity is seen corresponding to the repetition of the prism structure, as shown in Fig. 6. Note that the broad dip seen at around 10 mm on the y-axis in Fig. 6(b) is supposed to be due to the asymmetric arrangement of the dynodes. The fine variation may sometimes cause

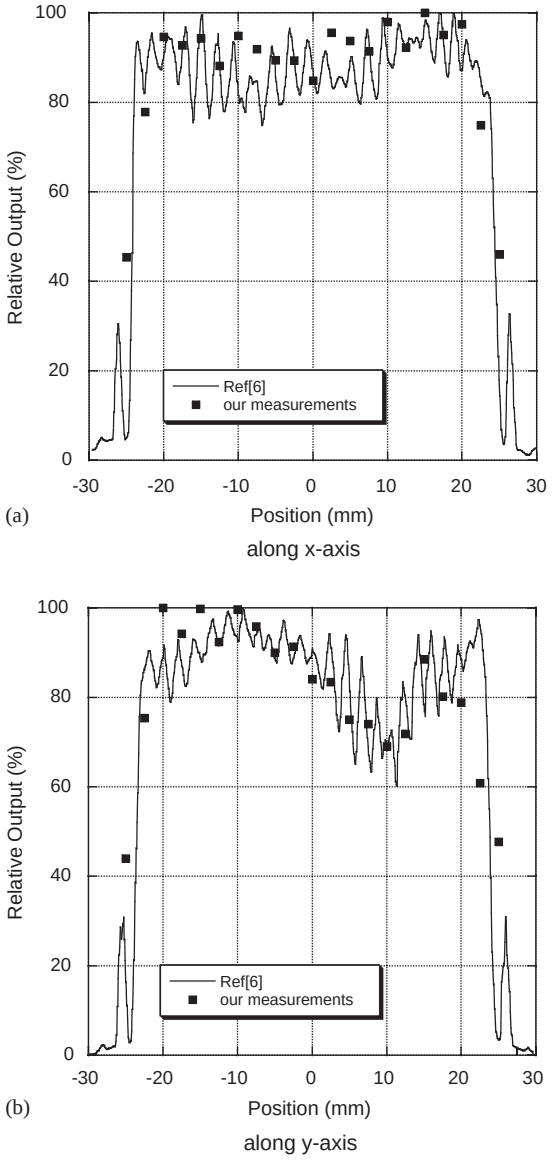

Fig. 6. Position dependence of the sensitivity for the new PMT (R329EGPX). The definition of the axes is the same as described in Fig. 7. The solid lines represent the data taken by Hamamatsu Photonics K.K. at 420 nm. The closed squares represent our data for the fiber readout with the WLS fiber of 1 mm in diameter.

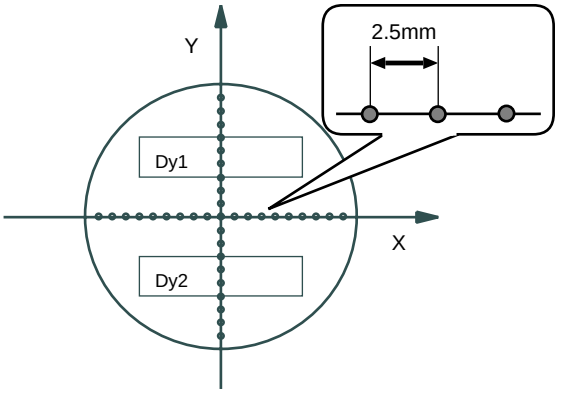

Fig. 7. Fiber positions of photon incidence in the measurement of TTD and uniformity.

problems, particularly when the fiber readout is applied. We studied the uniformity of the sensitivity for the fiber readout with the WLS fiber of 1 mm in diameter with the same setup employed for the photoelectron yield measurement. The fiber positions of the photon incidence are shown in Fig. 7. The measurements were carried out at the positions located along two lines, which are parallel and perpendicular to the dynode arrangement. Taking account of the interval of the repetition of the prism-structure, namely 1.5 mm, the pitch of the positions was chosen to be 2.5 mm. The behavior of our data, shown in Fig. 6, follows the data obtained by Hamamatsu Photonics K.K.. It also turned out that the fine variation was smeared out in the case of the fiber readout. Therefore, it will not cause any problem in our application for the lead-scintillator sandwich counters in E391a.

5. Time response

The time response is one of the important characteristics of PMTs. The prism-shaped photocathode, which gives a non-uniform electric field, may affect the time response. It can be observed in the electron transit time, the time for the electrons leaving from the photocathode to reach the anode. Usually, it strongly depends on the incident photon position on the photocathode. Photoelectrons emitted at different positions on the photocathode give different trajectories to the first dynode. Due to their low velocity, the different trajectories lead to a difference in the electron transit time, depending on the photon incident position. They also affect the spread in the electron transit time when the photocathode is uniformly illuminated.

5.1. Electron transit time difference (TTD)

We measured the TTD, the relative electron transit time, at different positions of photon incidence. The measurement was carried out using a pulse laser, Hamamatsu PLP-02, as shown in Fig. 8. It provides photons at a wavelength of 408 nm within a short duration of 58 ps. One of the positions on the photocathode was irradiated through a hole of 1.0 mm in diameter. The time difference between the synchronous trigger output of the pulse laser and the output signal of the PMT was measured by a TDC.

The data of TTD are shown in Fig. 9. The definition of the axes is the same as described in Fig. 7. The data sets along the x-axis show a more flat behavior compared with those along the y-axis. This is because the dynodes are symmetrically arranged along the x-axis. When we compared the results for the standard and new PMTs, the data set of the latter showed a zigzag behavior, which is supposed to be originated from the prism structure, although the data points of the standard PMT are smoothly connected. The data points of the latter ones spread over a slightly wider range than those of the former ones. However, the spreading is not significant and the overall

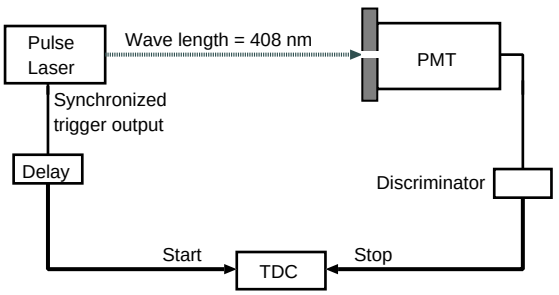

Fig. 8. Setup for the TTD measurement.

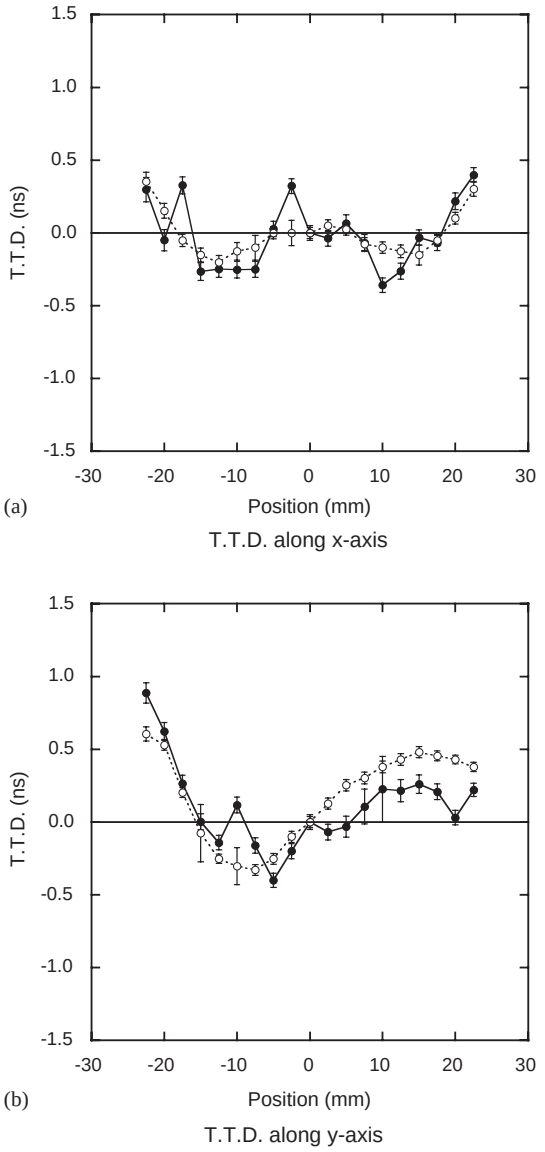

Fig. 9. TTD along (a) x-axis and (b) y-axis for the standard PMT (open circles) and the new PMT (closed circles). The PMTs are operated at 2.5 kV. The error bars are the root-mean-squares of the TDC distributions.

behaviors of the data for both PMTs are similar to each other.

5.2. Electron transit time spread (TTS)

The time response of PMTs can also be characterized by the TTS, the spread of the

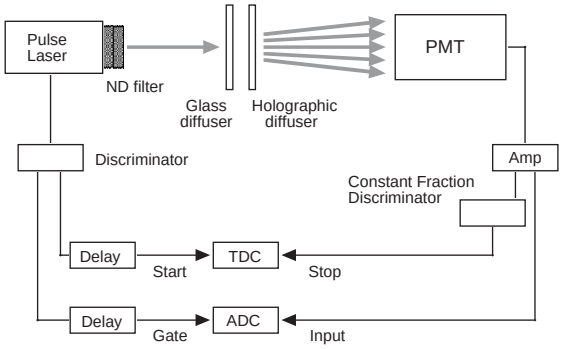

Fig. 10. Setup for the TTS measurement.

electron transit time. It is an important parameter, which dominates the time resolutions in time-of-flight counters as well as the number of scintillating photons. We evaluated the TTS by a measurement of the electron transit time for "single photoelectron events" under the condition that the whole surface area of the photocathode was uniformly irradiated by laser photons. Such a method is usually employed to obtain the catalog values of TTS by major suppliers of PMTs, including Hamamatsu Photonics K.K. [10].

The measurement setup is shown in Fig. 10. The laser beam, of which the intensity was significantly reduced by two filters,[2] was diffused by two optical diffusers[3] in such a way that only a few photons were incident on the photocathode with a uniform intensity distribution. We used the same pulse laser that was used in the TTD measurement. The time difference between the synchronous trigger output of the laser and the output of the PMT was registered by a TDC. We employed a constant-fraction discriminator for the PMT signal to eliminate the time spread due to the difference in pulse heights. Registering the PMT signal by an ADC, we selected only the "single photoelectron events" with a pulse height in the range of 1 ± 0.5 p.e..

The TDC distributions obtained with the standard and the new PMTs are shown in Fig. 11. We evaluated the spreads of the distributions in

[2] Products of Edmund Industrial Optics. The ND filters with transmittance of 0.3%.

[3] Products of Edmund Industrial Optics. The holographic diffuser and the opal glass diffuser.

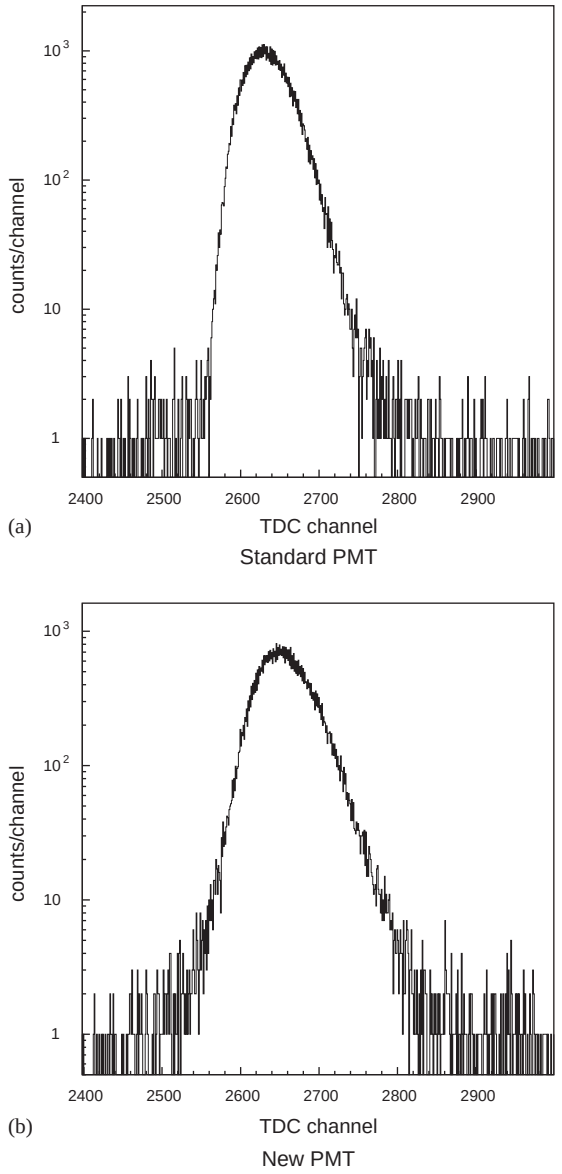

Fig. 11. TDC distributions obtained with (a) the standard PMT and (b) the new PMT. The scale of the horizontal axis is 25 ps/channel.

full-width at half-maximum (FWHM), as shown in Table 2. The standard PMTs gave 1.50 ns as the averaged value, while the new ones gave 1.89 ns. The observed spreads are reasonably supposed to be dominated by the TTS of the PMTs. And it is difficult to eliminate other small contributions to the spreads, e.g. difference in the photon path from the laser to the PMT, time spreads due to multiple scattering of the photons in the filters and the diffusers and so on. Thus, the observed spreads are regarded as upper limits of the TTS. Since the experimental conditions are the same, it can be stated that the new PMTs give a larger TTS than the standard PMTs. In other words, the time response of the new PMTs, investigated in the single photoelectron range, is significantly worse than that of the standard ones. However, in actual applications in TOF counters, their time resolutions are determined not only by the time response mentioned above, but also by the statistics of the photoelectrons. Thanks to the ability to give a better photoelectron yield of the new PMTs, their worse time response can be compensated so that the time resolutions of the TOF counters might be maintained.

Table 2
Time spreads observed in the TDC distributions

Type of PMT	Serial number	Spread (FWHM)
Standard PMTs (R329)	RD0292	1.69 ± 0.03 ns
	RD0644	1.39 ± 0.03 ns
	RD0717	1.44 ± 0.02 ns
	Average	1.50 ± 0.03 ns
New PMTs (R329EGPX)	ZK0679	1.90 ± 0.02 ns
	ZK0680	1.94 ± 0.03 ns
	ZK0682	1.82 ± 0.04 ns
	Average	1.89 ± 0.03 ns

6. Darkcurrent

It was of concern that the new PMTs have a problem due to the darkcurrent, for the following reasons:

(1) The photocathode surface area was extended by a factor of $\sqrt{2}$.
(2) The work function was lowered for an extended-green treatment.
(3) The electric field above the photocathode surface is locally strong, particularly, around the apex of the prisms.

An increase in the darkcurrent leads to a high threshold level, and spoils the efficiency of the

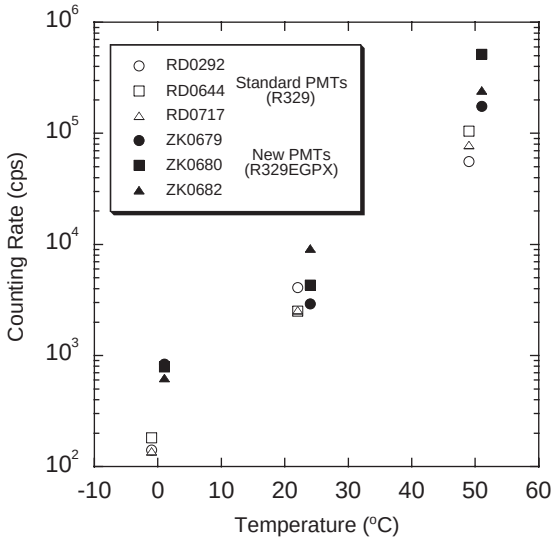

Fig. 12. Background noise counting rates as a function of the temperature in the darkcurrent measurement. The threshold voltage value corresponding to 0.5 p.e.. The open symbols denote the results for the original PMTs, and the closed symbols are for the new ones.

counters. We evaluated the darkcurrent at several temperatures (0°C, 23°C, 50°C) by measuring the counting rates at a threshold level of 0.5 p.e. with the PMTs not being irradiated. The results are shown in Fig. 12. We found that the new and the standard PMTs give similar darkcurrents at room temperature (23°C). In standard applications of the new PMTs, the darkcurrent is not a problem. At a higher temperature (50°C), the new PMTs give a few-times more darkcurrent than the standard ones. Therefore, when one wants to carefully avoid darkcurrent, their use at relatively low temperatures is recommended for the new PMTs, even in the room-temperature range. At a still lower temperature (0°C), the darkcurrent of the new PMTs is significantly reduced, by at most one order of magnitude compared with that at room temperature.

7. Conclusion

We have made improvements on the 2-in. PMT (Hamamatsu R329) to increase the photoelectron yield with a prism-shaped, an extended-green photocathode and polished electrodes. Consequently, about 1.8-times larger photoelectron yield was obtained with the new PMTs. A similar behavior in the TTD was found for the standard and new PMTs. However, the TTS of the new PMTs is significantly larger than that of the standard PMTs. The darkcurrent of the new PMTs is comparable to that of the standard PMTs at room temperature.

More extensive studies are required for the new PMTs, especially concerning the photoelectron yield at different photon incident angles. It is also desirable to improve the photoelectron yield in the short-wavelength region. Technical developments in making the prism structure will make it possible to employ a window material with better transmission. These changes will lead to new applications of the PMTs for calorimetry with scintillating crystals operated at shorter wavelengths. Another issue is an enlargement of the photocathode surface area, which is necessary for applications in Cherenkov counters.

Acknowledgements

We would like to thank Profs. S. Kato, H. Shimizu and the group members of Yamagata University, and all other E391a collaborators, for their discussions, encouragement and support. We are indebted to the engineers of Hamamatsu Photonics K.K. for their kind discussions concerning the PMTs.

References

[1] T. Inagaki, et al., Proposal of an experiment at the KEK 12 GeV proton synchrotron, Measurement of the $K_L^0 \to \pi^0 \nu\bar{\nu}$, KEK Int. 96–13 (1996) 1.
[2] K. Abe, et al., Contributed paper for ICHEP2000, Status of the $K_L^0 \to \pi^0 \nu\bar{\nu}$ Experiment at KEK (E391a), KEK preprint 2000–89, 2000.
[3] Yu.G. Kudenko, et al., Nucl. Instr. and Meth. A 469 (2001) 340–346.
[4] O. Mineev, et al., Nucl. Instr. and Meth. A 494 (2002) 362–368.
[5] Y. Yoshimura, et al., Nucl. Instr. and Meth. A 406 (1998) 435–441.

[6] Hamamatsu Photonics K.K. web catalog "R329-02_TPMH1254E01-1.pdf", available at http://www.hpk.co.jp/eng/products/ETD/pmte/pmt-ho2e.htm.
[7] Hamamatsu Photonics K.K., private communication.
[8] S. Yasumi, et al., Silica Aerogel Cherenkov Counter, KEK 83–25 (1984) 1.
[9] Hamamatsu Photonics K.K., Test report on $X-Y$ uniformity of R329EGPX #ZK0679, private communication.
[10] H. Kume (Ed.), Photomultiplier Tube—Basics and Applications, 2nd Edition, Hamamatsu Photonics K.K., Shizuoka, 1998, pp. 47–49.